



**UNIVERSITY
OF TURKU**

High Entropy Oxide Ceramics for Future Aerospace Thermal Barriers

Department of Mechanical and Materials Engineering
Bachelor's thesis

Author:
Ville Aronkytö

24.4.2025
Turku

The originality of this thesis has been checked in accordance with the University of Turku quality assurance system using the Turnitin Originality Check service.

Bachelor's thesis

Subject: Mechanical Engineering

Author(s): Ville Aronkytö

Title: High Entropy Oxide Ceramics for Future Aerospace Thermal Barriers

Supervisor(s): PhD Ashish Ganvir

Number of pages: 25 pages

Date: 24.4.2025

Thermal protection systems (TPS) are critical components in aerospace engineering, in re-entry vehicles (RVs) where extreme thermal and mechanical stresses occur during atmospheric re-entry. Contemporary TPS materials, such as reinforced carbon-carbon (RCC) and silica-based ceramics, have served well in the past missions to space. However, future aerospace applications demand enhanced thermal resistance, reusability, and environmental durability from the TPS. This thesis explores the potential of high entropy oxide ceramics (HEOCs) as next-generation thermal barrier materials.

HEOCs are a class of materials composed of multiple elements in near-equimolar ratios, leading to high entropy and stabilization of single-phase structures. These materials exhibit unique properties, including thermal stability (up to ~1600 °C), low thermal conductivity and improved mechanical performance due to entropy-driven effects, such as lattice distortion, cocktail effect and sluggish diffusion effects. A comparative analysis of selected HEOCs, particularly rare-earth zirconates and aluminium-based garnets was conducted against contemporary TPS materials. This highlighted their potential from moderate to high temperatures in aerospace environments depending on further application in the field.

The findings suggest that although HEOCs may not yet match the extreme temperature thresholds of current materials like the RCC, but the HEOCs studied exhibited a combination of thermal insulation, mechanical robustness, and structural tunability ranking them as promising candidates for future reusable thermal barrier applications.

Key words: High entropy oxide ceramics (HEOCs), Thermal protection systems (TPS), re-entry vehicles, thermal barriers, high entropy oxide, high entropy effect

List of used abbreviations:

TB Thermal Barrier

TPS Thermal Protection System

RV Re-entry Vehicle

NASA National Aeronautics and Space Administration

RCC Reinforced Carbon-Carbon

SiC Silicon Carbide

SSO	Space Shuttle Orbiter
HEO	High Entropy Oxide
UHTC	Ultra-High Temperature Ceramic
UHTCMC	Ultra-High Temperature Ceramic Matrix Composites
AI	Artificial Intelligence
CMC	Ceramic Matrix Composites
C/C	Carbon Reinforced Composites
C _f /C	Carbon Fabric Reinforced Composites
RLV	Reusable Launch Vehicle
HEOC	High Entropy Oxide Ceramics
BCC	Body-Centred-Cubic
FCC	Face-Centred-Cubic
TBC	Thermal Barrier Coating
NSGHE	$(\text{Nd}_{0.2}\text{Sm}_{0.2}\text{Gd}_{0.2}\text{Ho}_{0.2}\text{Er}_{0.2})_2\text{Zr}_2\text{O}_7$
LNSGH	$(\text{La}_{0.2}\text{Nd}_{0.2}\text{Sm}_{0.2}\text{Gd}_{0.2}\text{Ho}_{0.2})_2\text{Zr}_2\text{O}_7$
LNSGE	$(\text{La}_{0.2}\text{Nd}_{0.2}\text{Sm}_{0.2}\text{Gd}_{0.2}\text{Er}_{0.2})_2\text{Zr}_2\text{O}_7$
GYETYb	$(\text{Gd}_{0.2}\text{Y}_{0.2}\text{Er}_{0.2}\text{Tm}_{0.2}\text{Yb}_{0.2})_2\text{Zr}_2\text{O}_7$
YYbLEE	$(\text{Y}_{0.2}\text{Yb}_{0.2}\text{Lu}_{0.2}\text{Eu}_{0.2}\text{Er}_{0.2})_2\text{Al}_5\text{O}_{12}$

Table of contents

1	Introduction	5
1.1	Methodology	5
2	Literature review	7
2.1	History of Thermal Barriers in Aerospace Industry	7
2.2	Importance of Thermal Protection Systems	7
2.2.1	Aerodynamic Heating and Drag	7
2.2.2	Shape of the Re-entry Vehicle	8
2.3	Thermal Protection System Classification	9
2.3.1	Passive TPS	10
2.3.2	Semi-Passive TPS	11
2.3.3	Active TPS	11
2.4	Required Properties of Thermal Barriers	12
2.5	Thermal Barriers in Contemporary TPS	12
2.5.1	Carbon Reinforced Composites	13
2.5.2	Ultra-High Temperature Ceramics	13
2.5.3	Space Shuttle Orbiter TPSs	14
2.6	Overview of High Entropy Oxide Ceramics (HEOC)	15
2.6.1	Concept of Entropy	16
2.6.2	Core Characteristics of HEOCs	17
2.6.3	Structures of HEOCs	18
2.7	HEOC Properties	19
2.7.1	Example HEOCs	20
3	Discussion & Analysis	21
3.1.1	Comparison of Thermal Barriers	21
3.1.2	The Future in Terms of Thermal Barriers	22
4	Conclusions	23
5	References	24

1 Introduction

Thermal protection systems in aerospace applications require specific properties in the used materials. Thermal protection systems (TPS) should endure extremely high temperatures, oxidation, and could resist aerodynamic forces. All of which are present in the event of an atmospheric re-entry vehicle (RV). As is in the case of the National Aeronautics and Space Administration's (NASA's) Apollo program, during re-entry the shockwave plasma of the nose region reached temperatures ca. 10,727 °C at a speed of Mach 36 [1]. This is why TPS is essential in space vehicles specifically during the atmospheric re-entry phase of the flight [2].

Current challenges in TPS include environmental concerns, material development challenges, repairing difficulties regarding in-space repairs and self-healing TPS materials. Important factors in these materials are mass efficiency, reusability and material properties including thermal shock resistance and oxidation resistance. For example, in NASA Space Shuttle Orbiters (SSO), the nose cones and wing lead edges used TPS materials including reinforced carbon-carbon (RCC) coated with silicon carbide (SiC). The RCC is used to withstand temperatures up to 2400 °C and SiC coating is to prevent oxidation. [2]

The main goal is to determine whether high entropy oxide ceramics (HEOCs) could offer a solution to future thermal barriers. Ultra-high temperature ceramics (UHTC), ultra-high temperature ceramic matrix composites (UHTCMC) and structural oxide-based composites are already used in space engineering as TPS materials with promising results [2]. This lays the groundwork for possible uses regarding HEOCs as next-generation thermal barriers in thermal protection systems.

1.1 Methodology

In the making of this thesis AI tools, specifically ChatGPT, has been used to organize reference documents and find information within them using keywords. All text is produced without the help of an AI tool. AI has also been present in the making and arranging of the table of contents for this thesis.

Most of the sources were searched from ScienceDirect. Aerospace books on history, physics and journals online were also used. These documents help understand the topic in context and were searched online. Used keywords in the search include the following: thermal barriers, space shuttle, HEO, HEOC, TPS, atmospheric re-entry, high-entropy rare-earth etc.

Most sources used are published in the recent years. In newer topics, such as HEOCs the sources are published in the past five years. In the selection process of papers, a quick inspection of the paper, number of citations and date of publishing were done before deciding whether it should be a potential reference. These papers were then noted and categorized by relevance set by the table of contents.

Comparison of data and selection process of the materials in the thesis was made using the same process as mentioned above, with an addition of reading multiple papers on the materials and seeing the results section. A few of promising candidates were introduced in this thesis, regarding their found properties by their relevance in aerospace thermal protection systems.

2 Literature review

The goal of this literature review is to gain an overall understanding of the thermal barriers used in aerospace industry and the possible usage of high entropy oxide ceramics as thermal barriers in future aerospace or space shuttle applications.

2.1 History of Thermal Barriers in Aerospace Industry

In the 1950s and the 1960s it was believed that there is no material in existence to withstand the thermal heating in the re-entry process and so the term “thermal barrier” was introduced. In essence the thermal barrier (TB) or thermal protection system (TPS) is a system designed to protect the RV against aerodynamic heating encountered in the re-entry phase of the spaceflight. Many TPS technologies have been developed since to make RVs safer for re-entry. [2]

The first NASA space shuttle mission took place in April 1981 [3]. After the first mission numerous subsequent missions took place. All these missions contained a shuttle and were launched into an orbit around the earth. Space shuttles upon returning from the orbit during the re-entry phase encounter high temperatures with speeds around Mach 25 [1]. In terms of NASA’s shuttle program, the last mission took place in 2011 upon the retirement of the shuttle program [3]. NASA has since then stated in 2015 that more efficient TPS are required for future space missions [2].

2.2 Importance of Thermal Protection Systems

In general, the thermal protection systems are designed to prevent the RV, and the possible crew or cargo within, from aerodynamic heating damage. This heat shielding property should be accomplished without significantly increasing the weight of the protection system to keep the RV intact during the spaceflight. In addition, the TPS must be able to resist oxidation to function as a heat shield during atmospheric re-entry. [2]

2.2.1 Aerodynamic Heating and Drag

First an equation to gain a better understanding of the importance of heat protection in TPS regarding atmospheric RVs. Equation 1 defines aerodynamic heating as

$$q_w \approx \frac{1}{2} \rho_\infty V_\infty^3 C_H. \quad (1)$$

Where q_w is the heat flux [$\frac{W}{m^2}$], ρ_∞ is the freestream air density [$\frac{kg}{m^3}$], V_∞^3 is the freestream velocity [$\frac{m}{s}$] and C_H the heat transfer coefficient. The main idea presented in the equation 1 is that heat flux increases with the cube of the velocity of the vehicle. This means that aerodynamic heating caused by air friction increases rapidly during the re-entry phase when speeds reach Mach 25 as mentioned above. [1]

In addition to equation 1, equation 2 defines aerodynamic drag as

$$D = \frac{1}{2} \rho_\infty V_\infty^2 S C_D. (2)$$

Where D is the aerodynamic drag force [N], ρ_∞ and V_∞ are the same as in equation 1, S is the reference area [m^2] and C_D is the drag coefficient. As seen in equation 2, the aerodynamic drag increases with the square of the velocity of the vehicle. This means that the growth of aerodynamic heating is more rapid at high velocities than the growth of aerodynamic drag. [1]

2.2.2 Shape of the Re-entry Vehicle

In 1951 Ames laboratory started working on safe re-entry when H. Julian Allan coined his famous blunt body concept. In the concept Allan and Eggers from Ames approached heating issue in terms of the shape of the re-entry object. They found that a blunt body would not only generate a boundary layer between the object and shockwave, but also that the heat from friction was carried behind the blunt object by the shockwave. This resulted in a hot wake behind the blunt body and lower temperature levels on the body. [4]

The blunt body concept states that higher drag results in more heat dissipation into the atmosphere affecting the heat transfer into the re-entry vehicle [1]. The heat transfer for the vehicle is lower, since the blunt shape creates a larger shockwave that dissipates heat into the atmosphere more effectively than in a slender body or a cone structure [1]. The blunt body concept proven to be useful is not enough on its own. Even with the shape set on blunt body, the temperatures would still rise as high as 2760 °C in the blunt body [5].

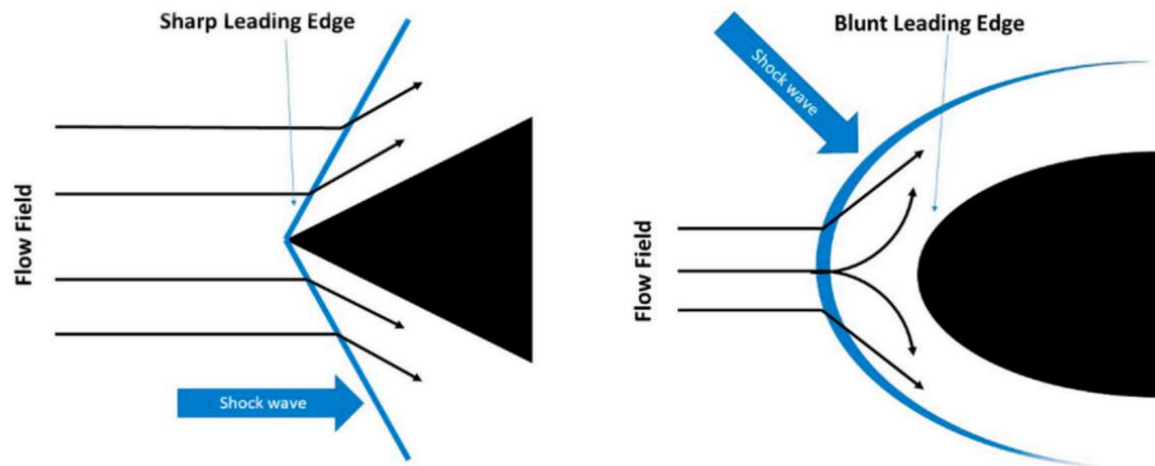


Figure 1: Spread of the shockwave of the leading-edge on blunt or sharp bodies reprinted with permission from [6].

The figure 1 above contains an illustration of the shape of the leading edge and the effect it has on the shockwave. On the right a blunt edge, the shockwave travels around the object carrying the shockwave to the wake along with the heat of friction [4], [6]. At this point it was getting clearer that a successful re-entry process would require a blunt body geometry and thermal properties from the materials that could withstand the ca. 2760 °C peak temperatures [2].

2.3 Thermal Protection System Classification

Thermal protection systems or thermal barriers can be classified into three concepts regarding methods of cooling down the structure and the vehicle by extension as well: passive TPS, semi-passive TPS and active TPS [2]. Example types of each classification will be included in the figure 2 below. In selecting between these TPS types mentioned in the figure 2 below, there are multiple factors to consider. These factors include type of propulsion system, geometry, heat flux amount on the surface and the exposure time of the surface [2].

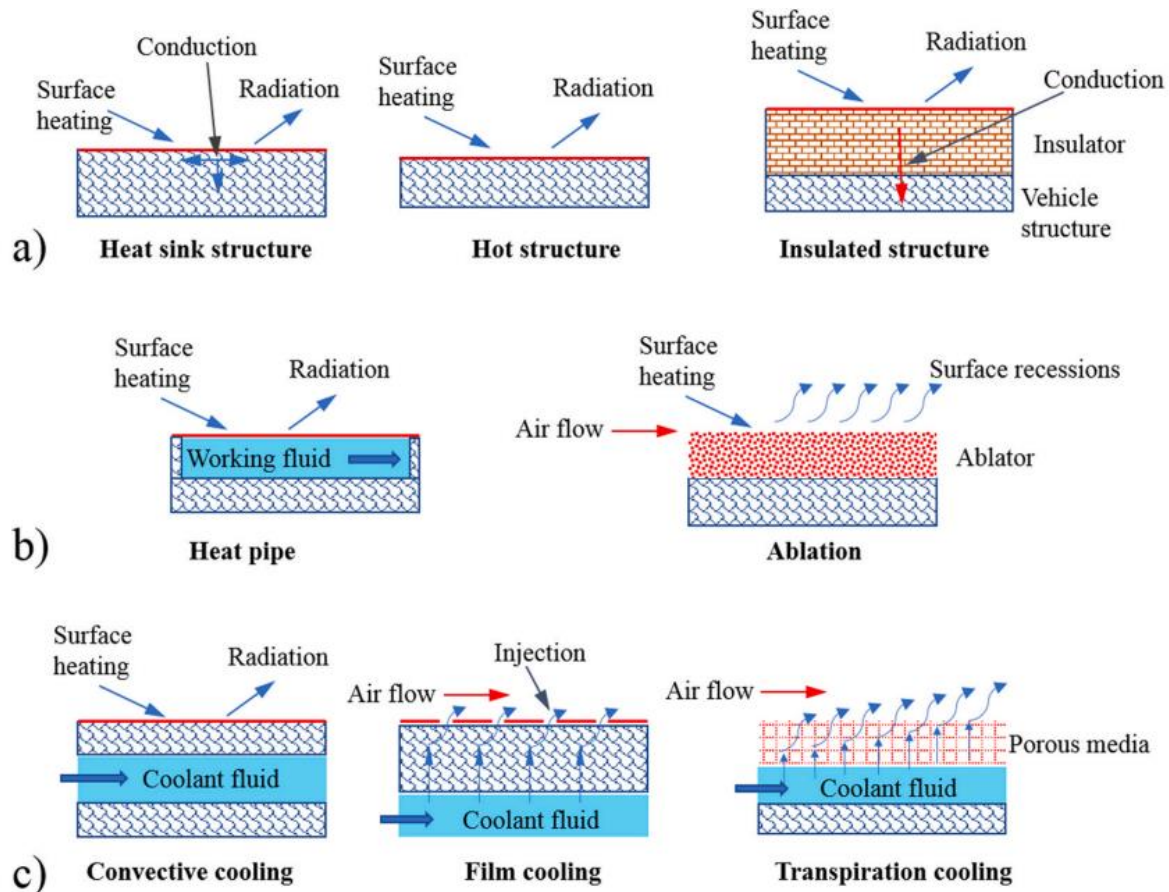


Figure 2: TPS Concepts in detail; a) Passive TPS, b) Semi-passive TPS, c) Active TPS reprinted with permission from [7].

2.3.1 Passive TPS

Passive TPS can be cooled with a heat sink, hot structure or an insulated structure like seen in figure 2. Heat sinks are generally used in cases where heat pulses are short. Heat sinks are typically made of a metal with high thermal storage capabilities. In hot structures emissivity is high and therefore re-radiation is high once the surface temperature reaches a certain point. Hot structures can withstand longer heat pulses than heat sinks, limiting factor being the temperature level itself. Insulated structures consist of two main layers. The outer layer is efficiently radiating heat to the surroundings while the inner layer insulates and slows down the transfer of heat. [2]

Passive TPS solutions are often reusable. Also, the temperatures in which passive TPS are used are as high as 1000 °C. In some instances, more than 1000 °C temperature must be endured, such as NASA's space shuttle orbiter (SSO). In the SSO the nose cap, lead edges and control surfaces encounter higher temperatures and require semi-passive or active TPS methods. For example, the conceptual X-33 spaceplane by NASA and Lockheed & Martin is

mostly cooled by passive TPS. Only exception to this being the nose cone and leading edges, which were planned to be passively or semi-passively cooled. [7]

2.3.2 Semi-Passive TPS

In semi-passive TPS heat pipes and ablative surfaces are used to cool down the system. Heat pipes transfer heat from intense heat areas to cooler areas using a working fluid in the process. Ablation is a concept where the surface of the material is disposable by nature and charring will occur at high temperatures. This char is relatively low level in strength, so it then vaporizes off the surface. Among many concepts ablation is considered promising and is still in use today. [2]

Most typical usage of semi-passive solutions is when moderate to high values of heat flux is encountered over a long period of time [7]. The nose cone and leading edges are often cooled by heat pipes in the RV [7]. Heat pipes in general are in the sequence of preference on the second place after passive solutions, and ahead of ablation and finally active solutions [7]. Ablation has been the most traditional approach to TPS and has been in use for over 40 years. In all NASA planetary entry probes hypersonic heating cases, ablative TPS was used [8]. Ablative surfaces designed to be single-use in most modern space capsules, but offer high heat flux resistance in exchange [7].

2.3.3 Active TPS

Active TPS is divided into transpiration cooling, film cooling and convective cooling. In convective cooling a cooling liquid is pumped under the surface of the TPS to achieve cooling of the vehicle. Film cooling is used in hypersonic vehicles, and it is based on the process of spraying a coolant film on the surface of the TPS. This way the coolant forms a film that cools the structure. In transpiration cooling a porous wall is used to transfer a coolant to the hot fluid side wall. While the coolant passes the porous wall the coolant absorbs heat and cools down the porous structure. This cooling results in a steady state and equilibrium state between the porous wall and the coolant. [2]

Transpiration cooling is used for extreme temperatures ≥ 1649 °C and longer flight times upwards of 1.5 hours [2]. Active cooling is considered least preferred of the choices. Active cooling contains higher weight, increased costs and has generally most complex structure. In some cases, active cooling is necessary, since it can sustain high heat flux. Usage of active

cooling is typical in space vehicles or RVs engine nozzles. In addition, leading edges of the space vehicle could be actively cooled if the exposure time is long and highest heat fluxes may reach $16 \text{ kW} / \text{cm}^2$. Heat fluxes greater than $1000 \text{ W} / \text{cm}^2$ are considered extremely high. [7]

2.4 Required Properties of Thermal Barriers

In the TPSs currently multiple factors must be taken into consideration. Hypersonic RVs are exposed to harsh aerodynamic environments during their flights [9]. The severity of these circumstances depends on the amount of time spent in these environments and the flights selected Mach number i.e. the speed of the RV during the mission [9]. Especially, the importance of reusability is paramount in the selection of TB materials [9].

The list of properties required for mostly reusable TPSs is long but can be summed in a seven-point list. The properties listed include high temperature capability (i), high temperature shock resistance (ii), stability over numerous missions (iii), high emissivity and low catalycity (iv), low thermal expansion (v), low thermal conductivity (vi), and minimal weight (vii). These are considered key properties of reusable TPS solutions in RVs and in reusable launch vehicles or RLVs. [2]

2.5 Thermal Barriers in Contemporary TPS

First a clarification between TPS and thermal barriers. Thermal Barriers are often the materials within the entirety of TPS, giving the system the heat resisting property. In this section the thermal barriers used in different TPS solutions is discussed. This overview into thermal barriers includes characteristics of different materials and usage. A closer look at the TPSs in the Space Shuttle Orbiter (SSO) is also presented in this section.

In reusable TPS applications, materials such as the Inconel superalloy, carbon reinforced composite (C/C) and silica fibre ceramic tiles were used in the 20th century TPSs against re-entry heating [7]. In the 21st century reusable TPSs materials include ultra-high temperature ceramics (UHTCs), multiple carbon and silicon carbides mixed with ceramic matrix composites (CMCs) and lightweight superalloys [7]. Recently UHTCs have been tested for TPS applications with promising results [2].

2.5.1 Carbon Reinforced Composites

Carbon reinforced composites (C/C) are used in thermal barriers and therefore in TPS, specifically in nose cones and lead edges of RVs [7]. Benefits of C/C composites include low density ($\rho \leq 2.0 \frac{g}{cm^3}$), high corrosion resistance, low thermal expansion coefficient, thermal shock resistance and high material strength [10]. In oxygen-present environments and at high temperatures C/C composites alone are rarely utilized, since oxidation occurs only at above 400 °C [10].

One of the earliest material examples of C/C composites is reinforced carbon-carbon (RCC), which was developed in the 1960s. Reinforced carbon-carbon is a C/C composite, in which the carbon reinforced composite is coated with silicon carbide (SiC). With the SiC coating the RCC is much more resistant to oxidation at above 500 °C and able to withstand temperatures up to 2400 °C. This SiC coating on the RCC acts as a separate layer and offers protection on the material strength as well. [2]

2.5.2 Ultra-High Temperature Ceramics

Temperatures reaching over 1600 °C and even above 2200 °C are categorized as ultra-high temperatures [11]. Research on the UHTCs started in the 1950s since their innate ability to resist corrosion at high temperatures [6]. UHTCs were considered an interesting topic already in the 1960s widely across aerospace applications, with research still continuing today [6]. Disregarding the temperatures, ultra-high temperature ceramics (UHTCs) must be able to withstand high heat flux, mechanical stress and vibrations during the launch sequence or the re-entry phase of the RV [11].

UHTCs showed in experiments by Ames Glenn Research Centre and Air Force Space Command to be brittle and shatter [6]. In addition, the UHTCs showed to have important traits when it comes to ablation resistance in difficult environments [6]. To overcome this brittleness in UHTCs there have been numerous attempts, one of which was toughening the bulks of structures with continuous fibres [6]. In effect, the improvement of brittleness and thermal shock resistance can be seen in the study of ultra-high temperature ceramic matrix composites (UHTCMCs) [6].

The innate brittleness is yet to overcome in UHTCMCs, the overall brittleness of the composite is improved largely with the introduction of continuous fibre-reinforcement [6].

Ultra-high temperature ceramics (UHTCs) and ultra-high temperature ceramic matrix composites (UHTCMCs) are significantly different from one another [2]. It is believed that UHTCMCs are more resistant to oxidation, fractures and thermal shock than UHTCs in general [2].

Carbon ceramic composites have become a promising area in the study regarding UHTC thermal barriers in aerospace heat-shields [12]. One of such materials is C_f/C-UHTC carbon fabric composite [12]. This composite often contains differing amounts of SiC in the matrix [12]. In this case, the composite matrix system consisted of HfC–HfB₂–NbC–NbB₂–TiC–TiB₂–B₄C–SiC, with the quantity of SiC in the system not exceeding 9.0 wt% [12]. The results indicated that said C_f/C-UHTC has potential in high temperature applications, and further research toward different compositions was encouraged as well [12].

2.5.3 Space Shuttle Orbiter TPSs

In understanding the thermal protection systems of any reusable launch vehicles (RLVs) in general, figure 3 below is to illustrate the TPS solutions in NASAs Space Shuttle Orbiter (SSO). The first mission (STS-1) of the SSO flight was a test mission by nature and it was launched in April, 1981 [3]. Whilst material selection was made on the SSO, the TPSs were supposed to be mostly reusable [2]. The overall structure of the SSO was aluminium and the TPS solutions were bonded to the surface of the vehicle [2].

Five basic materials were selected, and they are seen in figure 3 below [2]. These materials are reinforced carbon-carbon, high-temperature reusable surface insulation tiles, low-temperature reusable surface insulation tiles, advanced flexible reusable surface insulation blanket, and flexible reusable surface insulation blanket.



Figure 3: Different thermal protection systems used in the initial SSO design; different materials are assigned different colours for easier recognition. Figure reprinted from [2] with permission.

Highest re-entry heating areas are protected by specially processed RCC material and covered with SiC coating to prevent oxidation [13]. High-temperature reusable surface insulation (HRSI) tiles and low-temperature reusable surface insulation (LRSI) tiles were widely used in the SSO initially [2]. LRSI tiles and HRSI tiles main differences include the colour of the material and by extension the reflectivity. LRSI tiles were coated white, making them more reflective than HRSI tiles. LRSI tiles were there to maintain temperatures at around 694 °C. HRSI tiles, which were made of black borosilicate glass coating, maintained temperatures at around 1260 °C. The RCC coated with SiC was developed in the 1960s. The HRSI and LRSI tiles were developed in the 1970s. [2]

Later, in the 1980s the advanced flexible reusable surface insulation blankets (AFRSI) and more common flexible reusable surface insulation blankets (FRSI) were introduced. FRSI blankets kept temperatures below 370 °C and AFRSI blankets temperatures were higher at around 650 °C. In the initial SSO TPS design LRSI tiles were commonly used but later NASA decided to replace the LRSI tiles with AFRSI blankets. AFRSI blankets were considered better alternatives due to their lighter weight and stronger structure than LRSI tiles. [2]

2.6 Overview of High Entropy Oxide Ceramics (HEOC)

The scientific research has been increasing regarding high entropy oxide ceramics (HEOCs) in the past years [14]. In moving towards HEOCs it is important to understand the concept of

entropy and the properties or characteristics of high entropy materials (HEMs). In general, high entropy materials consist of five or more elements in the same or nearly the same molar ratios [15]. High levels of chemical complexity alongside crystal structures are introduced into this multi-element system making the final material show its one-of-a-kind chemical and physical properties [15]. The studying of high entropy materials began with high entropy alloys (HEAs) in 2004 [15].

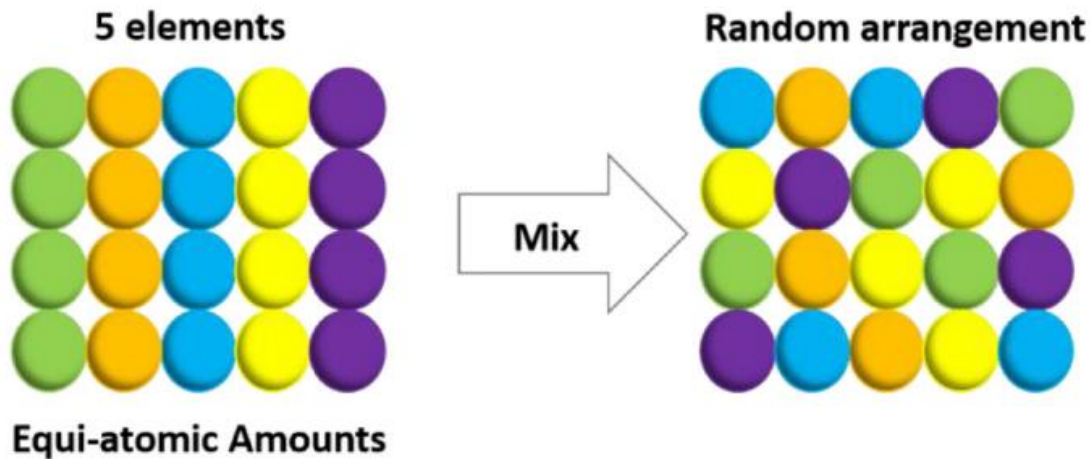


Figure 4: Showing atomically equal quantity of elements before and after mixing. Reprinted with open-access from [16].

2.6.1 Concept of Entropy

Entropy as a concept was introduced in 1850 by a German physicist, Rudolf Clausius [14]. In the concept entropy is defined as the degree of disorder in a thermodynamic system, and this initial degree of disorder is used to determine the disorder of the entire system [14]. In cases where the system has high entropy, the entropy calculation is important [14]. The following equation (3) shows the calculation of mixing entropy of HEOs in an ideal state:

$$\Delta S_{mix} = -R \sum_{N=1}^{i=1} x_i \ln x_i. \quad (3)$$

In the eq. (3) above R is the gas constant ($R = 8.314 \frac{J}{K \cdot mol}$), x_i is the atomic fraction of i th element and N being the total number of elements. As seen in the eq. (3) the mixing entropy (ΔS_{mix}) reaches maximum value when atomic fraction is equal, and number of elements is high. This equation can be further simplified for cases with equal atomic compositions. [14], [17]

$$\Delta S_{mix} = R \ln N. (4)$$

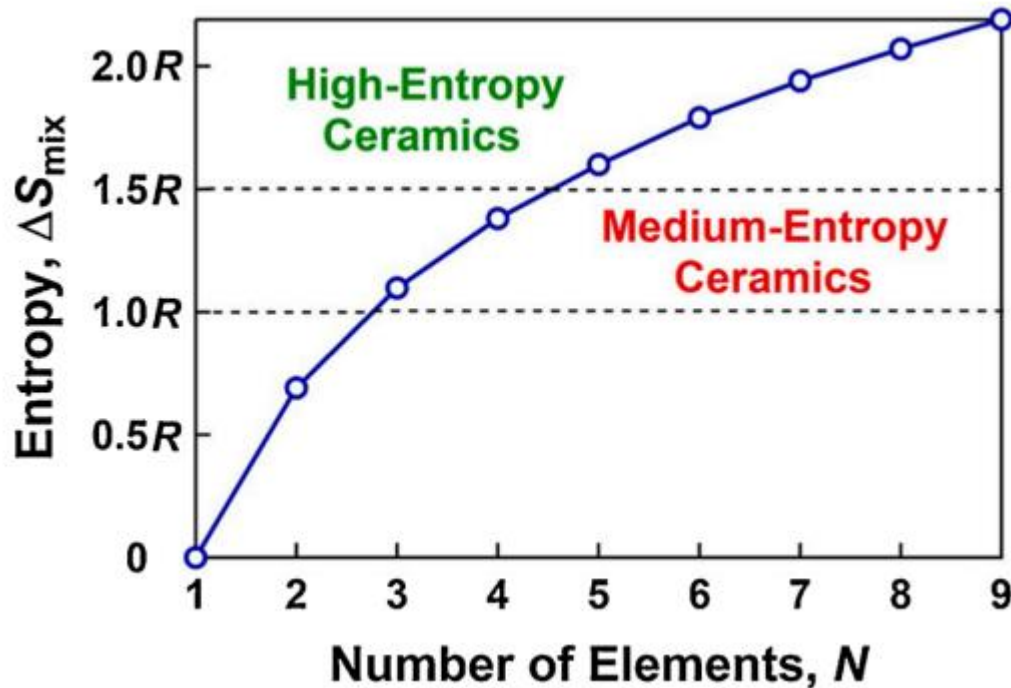


Figure 5: Definitions of high-entropy ceramics and medium-entropy ceramics, and relations between mixing entropy and number of elements. Reprinted with permission from [17].

The effect of element number on the entropy of mixing in equal atomic mixtures calculated with eq. (4) is seen in the figure 5 above to further demonstrate the idea. It is seen in the figure 5 above that raising the entropy results in simpler forming and stabilizing of single-phase materials with multiple mixed elements within [17]. This fig. 5 shows that for a material to be considered high in entropy, at least 5 elements are required in the mix. In addition, a mixing entropy value ($\Delta S_{mix} > 1.5 R$) confirms the materials high entropy status.

2.6.2 Core Characteristics of HEOCs

The HEOCs can be characterized by four core effects: (i) High entropy effect, (ii) Severe lattice distortion effect, (iii) Sluggish diffusion effect, and (iv) Cocktail effect [18]. These four characteristics are the result of the powerful mixing nature within the materials in HEOCs [18].

The high entropy effect (i) is one of the main features in HEMs [15]. In short, this effect increase the mixing disorder, which in turn lowers the overall energy of the material [15].

This results in preventing the atoms from separating or forming multiple phases, which helps the material keep a steady single phase even in complex chemical environments [15].

Severe lattice distortion effect (ii) in short happens when atoms of different sizes and properties distort the crystal structure. In terms of HEOCs, metal and oxygen ions are spread evenly throughout the structure. When atom size or the bonding behaviour is altered, irregularities in the crystal structure will ensue. While irregularities increase the chances of distortions and dislocations, this could lead to noticeable local lattice distortions. [15]

The sluggish diffusion effect (iii) is the result of different diffusion rates of elements and the high entropy effect. In HEMs atoms can only move (diffuse) when there are suitable vacancies in the lattice. In the case of HEOCs, lattice distortion and interactions between atoms lead to each atom getting slightly moved from its ideal position. This then raises the material's energy and reduces the moving of atoms. Resulting in slower diffusion. At higher temperatures slower diffusion is useful, since it improves the phase stability of HEOCs. [15]

The cocktail effect (iv) is a descriptive name for an effect in HEOCs coined by an Indian researcher Ranganathan in 2003. As the name suggests, the simple combination of elements' properties is not the full result of the material. Elements interact in complex ways to create new and possibly better properties when mixed. The name of the effect is inspired by the synergistic nature of cocktails, the combination of ingredients often results in better outcome than ingredients on their own. [15], [18]

2.6.3 Structures of HEOCs

Properties such as strength and hardness of HEAs is mostly determined by the structure of a given HEA [19]. These structures include body-centred-cubic (BCC) or face-centred-cubic (FCC) structures [19]. In BCC-structured HEAs plasticity is limited and yield strength is low [19]. Mixing both BCC and FCC structures is often necessary to achieve desirable mechanical properties, such as high strength and good ductility [19]. Since HEOCs have multiple elements compared to traditional ceramics, the structure is often a complex crystal structure [14].

In HEOCs a myriad of different crystal structures are known, which include rock-salt, fluorite, perovskite, spinel, pyrochlore, and olivine structures [14]. Of these structures, rock-salt type structures are one of the most studied, since it was discovered early and formation of the structure is considered easy [15]. In rock salt type structures, the $(\text{MgCoNiCuZn})\text{O}$ is the

most classic example [15]. This rock salt type structure of HEOC has been the base for the following rock salt type structures that have been found [15]. Rock salt is a basic crystal structure overall, which is common in HEOs [14]. HEOCs with this rock salt structure exhibit properties such as high ionic conductivity and high dielectric constant [14].

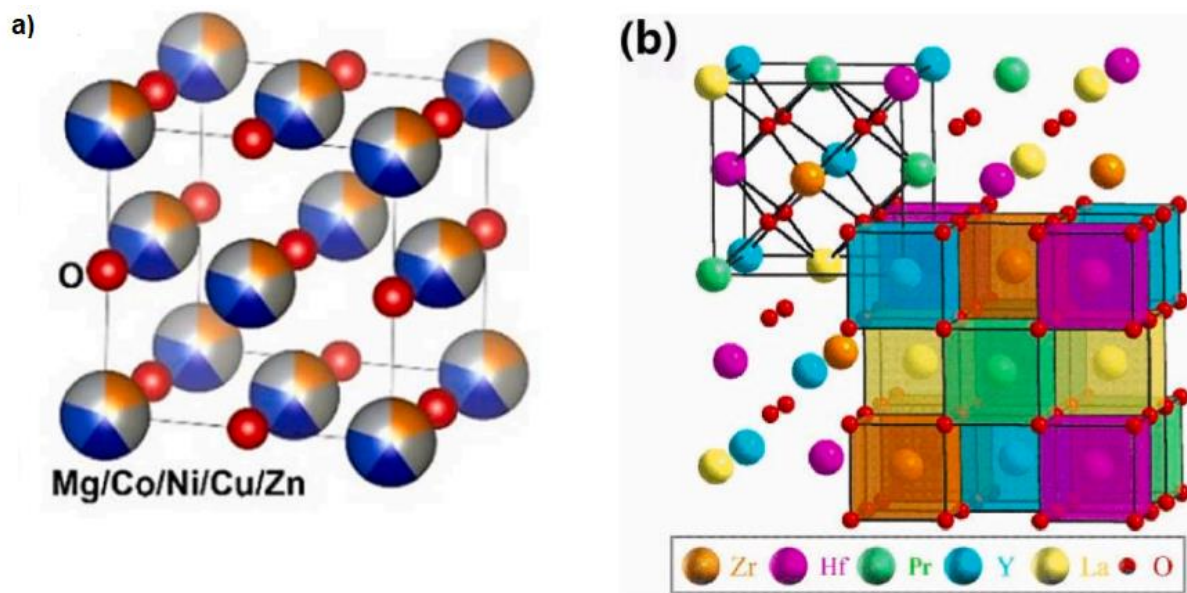


Figure 6: Showing the crystal structure of rock salt type HEOCs (a) and crystal structure of fluorite type HEOCs (b). Reprinted with open-access from [15].

Another crystal structure of HEOCs is fluorite. After the entropy-stabilized rock salt type structures were introduced, entropy's effects on different oxide structures was researched further [14]. Multiple rare-earth oxides with fluorite structures emerged with functional properties of high value [14]. The concept of entropy has also provided new possibilities in designing and synthesizing these structures [14].

2.7 HEOC Properties

In general, HEOCs possess diverse properties, which are potentially valuable for multiple fields of research, including thermal barrier coatings (TBCs) [14]. Some of these valuable properties are good thermal stability and high hardness [20]. HEOCs have also been noticed to reduce thermal conductivity, which is of value in thermal barrier coating [20]. Studies of HEOCs as TBC materials have been conducted increasingly in the past years [20].

2.7.1 Example HEOCs

Some potential HEOCs could include high entropy rare-earth zirconate ceramics. A selection of three of these said HEOCs are: $(\text{Nd}_{0.2}\text{Sm}_{0.2}\text{Gd}_{0.2}\text{Ho}_{0.2}\text{Er}_{0.2})_2\text{Zr}_2\text{O}_7$ (NSGHE), $(\text{La}_{0.2}\text{Nd}_{0.2}\text{Sm}_{0.2}\text{Gd}_{0.2}\text{Ho}_{0.2})_2\text{Zr}_2\text{O}_7$ (LNSGH), and $(\text{La}_{0.2}\text{Nd}_{0.2}\text{Sm}_{0.2}\text{Gd}_{0.2}\text{Er}_{0.2})_2\text{Zr}_2\text{O}_7$ (LNSGE) [21]. These HEOCs altogether exhibited high thermal expansion coefficients ($11.20\text{--}11.69 * 10^{-6} * \text{K}^{-1}$ at $1200\text{ }^\circ\text{C}$) and low thermal conductivity at room temperature [21]. The HEOCs also exhibited excellent mechanical properties such as hardness ($8.746\text{--}11.259\text{ GPa}$) and fracture toughness [21].

Other candidate exhibiting promising properties in HEOCs include another high entropy rare-earth zirconate ceramic, $(\text{Gd}_{0.2}\text{Y}_{0.2}\text{Er}_{0.2}\text{Tm}_{0.2}\text{Yb}_{0.2})_2\text{Zr}_2\text{O}_7$ (GYETYb) [22]. Exhibiting extremely low thermal conductivity, high thermal expansion coefficient ($10.61 * 10^{-6} * \text{K}^{-1}$ at $1300\text{--}1400\text{ }^\circ\text{C}$) and also excellent mechanical properties [22]. These mechanical properties include hardness (11.98 GPa), elastic modulus and fracture toughness [22].

Last one of selected HEOC candidates is a high entropy aluminium-based oxide ceramic, $(\text{Y}_{0.2}\text{Yb}_{0.2}\text{Lu}_{0.2}\text{Eu}_{0.2}\text{Er}_{0.2})_2\text{Al}_5\text{O}_{12}$ (YYbLEE) [23]. The thermal expansion coefficient is relatively low at $(8.54 \pm 0.29) * 10^{-6} * \text{K}^{-1}$ at $400\text{--}1000\text{ }^\circ\text{C}$ and the thermal conductivity is relatively high [23]. The HEOC (YYbLEE) is still a promising candidate for thermal barrier applications [23].

3 Discussion & Analysis

This literature review was set out to explore whether high entropy oxide ceramics (HEOCs) could be seen as a viable alternative to traditional thermal protection system (TPS) materials or i.e. thermal barriers. This goal was set by the importance of TPS in re-entry vehicles (RVs). In short TPS consisting of thermal barriers is essential in RVs because of the intense heating during re-entry and the aerodynamic forces acting on the RV.

3.1.1 Comparison of Thermal Barriers

Table 1: Comparison of properties between HEOCs, C_f/C-UHTC and contemporary thermal barriers.

TPS Material	Density (kg / m ³)	Maximum Operating Temperatures (°C)	Thermal Conductivity (W / m*K)	Elastic Modulus (GPa)	Fracture Toughness (MPa * m ^{0.5})
RCC, SiC coating	1600–1980	2400	690	40–100	5–10
LRSI	140	650	0.048	-	3
HRSI	144	1260	0.126	-	3
AFRSI	145	650	-	-	-
C _f /C-UHTC	2790–2910	1500*	0.280–0.285	7.8 ± 0.2	-
(NSGHE)	6952 (theoretical)	~1600**	1.996 at ~23 °C	-	0.990
(LNSGH)	6672 (theoretical)	~1600**	1.976 at ~23 °C	-	1.196
(LNSGE)	6617 (theoretical)	~1600**	1.745 at ~23 °C	-	2.382
(GYETYb)	7023 (theoretical)	< 1400	0.82 at 1200 °C	178	1.5352
(YYbLEE)	6010 (theoretical)	~1590***	3.81 at ~27 °C	-	-

In this table some relevant properties of known thermal barriers are compared to selected HEOCs properties. Properties of HRSI, LRSI, RCC, AFRSI derived from [2]. Properties of C_f/C-UHTC from [12]. Properties of (NSGHE), (LNSGH) and (LNSGE) from [21]. Properties of (GYETYb) from [22]. Properties of (YYbLEE) from [23]. HEOCs in tan, SSOs TPSs in white and C_f/C-UHTC in gray background for visual enhancement.

* = Si₃N₄ -component of the C_f/C-UHTC, maximum stable temperature is 1500 °C [12].

** = 40 hours of heat treatment at 1600 °C and remained stable [21].

*** = 18 hours of heat treatment at 1590 °C and remained stable [23].

In table 1 above a comparative summary of the material properties for different TPS candidates is presented. This includes traditional ceramics, UHTCs and HEOCs. The materials are assessed based on the key performance metrics most relevant to re-entry applications: density, maximum operating temperature, thermal conductivity, elastic modulus, and fracture toughness. Abbreviations are used in the table below for convenience.

As seen in the table 1 above, many values differ from each other, which is the result of different sources being used and their varying way of categorizing values. All properties in the table are considered important in the use of TPS in general. Regarding HEOCs experimental data is limited since the research field is relatively new and has been pivoting in recent years showed by an increase in number of published papers.

From the table 1 above it is clear that RCC coated with SiC is exhibiting the highest peak temperature capabilities ca. 2400 °C, but HEOCs such as NSGHE, LNSGH and LNSGE demonstrate promising maximum stability in temperatures ca. 1600 °C, suggesting their potential in moderate to high temperature applications within thermal barriers. HEOCs in general also exhibit lower thermal conductivity than RCC, but higher than classic silica tiles such as LRSI and HRSI. Indicating promising stiffness, GYETYb with 178 GPa is by far the most advanced in the comparison, further demonstrating the capabilities of HEOCs.

In short, although the HEOCs do not reach the ultra-high thermal thresholds of RCC, the combination of moderate density range, mechanical structure, and ductility through entropy design makes them highly promising for next generation of thermal barriers in aerospace applications. HEOCs are relatively new in the field of thermal barriers and should be researched more.

3.1.2 The Future in Terms of Thermal Barriers

Future prospects in aerospace applications include interplanetary travel in manned missions [2]. These missions would require significantly more from the thermal barriers in TPS solutions seen today. Flight times would be increased in addition to sustainable reusability of the RVs. This sets the stage for more demanding requirements of thermal barriers for the future. When missions to new planets arise, new properties may be needed from thermal barriers. For example, Venus has a vastly different atmosphere than Earth has, so it is another factor to consider when new thermal barriers are designed.

4 Conclusions

The scope of this thesis was to explore the usage of high entropy oxide ceramics in thermal barriers, in aerospace re-entry applications particularly. The extreme temperatures in the re-entry phase alongside high aerodynamic stresses make the thermal protection of the vehicle mandatory. This demands also other properties from the materials in question, such as mechanically robust and stable materials with resistance to oxidation. In best case scenario these materials should also be reusable.

In this literature review some of current materials were explained in more detail, such as RCC and UHTCs. Key points from these material overviews provided insight towards the strengths and limitations of current thermal barriers. For example, RCC withstanding high temperatures up to 2400 °C but suffering from relatively high density and oxidation issues without a proper coating applied to it. In contrast, HEOCs are offering a new route with the help of high entropy effect and the cocktail effect, to have more favourable thermal and mechanical properties in the future.

Through this literature review and the comparison of materials, findings regarding rare-earth zirconate HEOCs such as NSGHE, LNSGH, and LNSGE exhibited quite high thermal stability at 1500–1600 °C, with relatively low thermal conductivity and promising fracture toughness. Aluminium based garnet type HEOC such as YYbLEE on the other hand demonstrated strong structural integrity and potential for multifunctional applications.

While the characteristics of HEOCs are promising, the HEOCs are still majorly experimental. A long-term validation is required under realistic or concrete aerospace conditions. Challenges with the complications of the synthesis process of these materials and the sheer volume of possibilities. Most of the research regarding the HEOCs is done with five elements and increasing the number of elements the number of possible mixes grow exponentially. This opens doors and studying further is important.

In short, HEOCs are offering a new direction in the development of next-generation thermal barriers in many industries, including aerospace industry. To unlock the full potential of HEOCs in re-entry vehicles, more research on the matter is needed. The foundation laid by this review indicates strong potential of HEOCs to complement or even replace thermal barriers in the upcoming aerospace missions.

5 References

- [1] J. D. Anderson Jr., *Hypersonic and High Temperature Gas Dynamics*, 2nd ed., vol. 2006. in AIAA Education Series, vol. 2006. Blacksburg, Virginia, USA: AIAA, Inc., 2006.
- [2] O. Uyanna and H. Najafi, “Thermal protection systems for space vehicles: A review on technology development, current challenges and future prospects,” *Acta Astronaut.*, vol. 176, pp. 341–356, Nov. 2020, doi: 10.1016/j.actaastro.2020.06.047.
- [3] J. M. Lafleur and J. H. Saleh, “Survey of mission evolution and flexibility in the Space Shuttle program,” *Space Policy*, vol. 26, no. 4, pp. 236–245, Nov. 2010, doi: 10.1016/j.spacepol.2010.08.006.
- [4] G. E. Bugos, *Atmosphere of Freedom: Sixty Years at the NASA Ames Research Center*. National Aeronautics and Space Administration, NASA History Office, 2000.
- [5] R. D. Launius and D. R. Jenkins, *Coming Home: Reentry and Recovery from Space*. Government Printing Office, 2012.
- [6] Maryam Shojaie-bahaabad, M. Bozorg, M. Najafizadeh, and P. Cavaliere, “Ultra high temperature ceramic coatings in thermal protection systems (TPS),” *Ceram. Int.*, vol. 50, no. 7, Part A, pp. 9937–9951, Apr. 2024, doi: 10.1016/j.ceramint.2023.12.372.
- [7] V. T. Le, N. S. Ha, and N. S. Goo, “Advanced sandwich structures for thermal protection systems in hypersonic vehicles: A review,” *Compos. Part B Eng.*, vol. 226, p. 109301, Dec. 2021, doi: 10.1016/j.compositesb.2021.109301.
- [8] G. Pulci, J. Tirillò, F. Marra, F. Fossati, C. Bartuli, and T. Valente, “Carbon–phenolic ablative materials for re-entry space vehicles: Manufacturing and properties,” *Compos. Part Appl. Sci. Manuf.*, vol. 41, no. 10, pp. 1483–1490, Oct. 2010, doi: 10.1016/j.compositesa.2010.06.010.
- [9] J. J. Bertin and R. M. Cummings, “Fifty years of hypersonics: where we’ve been, where we’re going,” *Prog. Aerosp. Sci.*, vol. 39, no. 6, pp. 511–536, Aug. 2003, doi: 10.1016/S0376-0421(03)00079-4.
- [10] Y. Zhou *et al.*, “Ablation behavior of C/C composite matrix-modified with solid solution ceramic TaZr₂C₃–SiC under an oxyacetylene flame,” *J. Mater. Res. Technol.*, vol. 36, pp. 1362–1378, May 2025, doi: 10.1016/j.jmrt.2025.03.102.
- [11] S. Tang and C. Hu, “Design, Preparation and Properties of Carbon Fiber Reinforced Ultra-High Temperature Ceramic Composites for Aerospace Applications: A Review,” *J. Mater. Sci. Technol.*, vol. 33, no. 2, pp. 117–130, Feb. 2017, doi: 10.1016/j.jmst.2016.08.004.
- [12] A. N. Astapov, V. A. Pogodin, I. V. Sukmanov, B. E. Zhestkov, and M. V. Prokofiev, “Development of Cf/C-UHTC composite and study of its resistance to oxidation and ablation in high-speed high-enthalpy air plasma flow,” *Int. J. Lightweight Mater. Manuf.*, vol. 7, no. 3, pp. 362–377, May 2024, doi: 10.1016/j.ijlmm.2024.02.003.
- [13] K. H. Lyle and E. L. Fasanella, “Permanent set of the Space Shuttle Thermal Protection System Reinforced Carbon–Carbon material,” *Compos. Part Appl. Sci. Manuf.*, vol. 40, no. 6, pp. 702–708, Jul. 2009, doi: 10.1016/j.compositesa.2009.02.016.
- [14] Y. Jiao *et al.*, “Overview of high-entropy oxide ceramics,” *Mater. Today*, vol. 77, pp. 92–117, Aug. 2024, doi: 10.1016/j.mattod.2024.06.005.
- [15] G. Du *et al.*, “Research progress on high entropy oxide ceramics: Principles, preparation, and properties,” *J. Mater. Res. Technol.*, vol. 35, pp. 265–288, Mar. 2025, doi: 10.1016/j.jmrt.2025.01.015.
- [16] S. H. Albedwawi, A. AlJaberi, G. N. Haidemenopoulos, and K. Polychronopoulou, “High entropy oxides-exploring a paradigm of promising catalysts: A review,” *Mater. Des.*, vol. 202, p. 109534, Apr. 2021, doi: 10.1016/j.matdes.2021.109534.
- [17] S. Akrami, P. Edalati, M. Fuji, and K. Edalati, “High-entropy ceramics: Review of principles, production and applications,” *Mater. Sci. Eng. R Rep.*, vol. 146, p. 100644, Oct. 2021, doi: 10.1016/j.mser.2021.100644.
- [18] M. Anandkumar and E. Trofimov, “Synthesis, properties, and applications of high-entropy oxide ceramics: Current progress and future perspectives,” *J. Alloys Compd.*, vol. 960, p. 170690, Oct. 2023, doi: 10.1016/j.jallcom.2023.170690.

- [19] Y. Zhang *et al.*, “Microstructures and properties of high-entropy alloys,” *Prog. Mater. Sci.*, vol. 61, pp. 1–93, Apr. 2014, doi: 10.1016/j.pmatsci.2013.10.001.
- [20] L. Cong, W. Li, J. Wang, S. Gu, and S. Zhang, “High-entropy (Y_{0.2}Gd_{0.2}Dy_{0.2}Er_{0.2}Yb_{0.2})₂Hf₂O₇ ceramic: A promising thermal barrier coating material,” *J. Mater. Sci. Technol.*, vol. 101, pp. 199–204, Feb. 2022, doi: 10.1016/j.jmst.2021.05.054.
- [21] S. Zhao, Z. Wang, J. Cao, W. Wang, and W. Wen, “Study on high-entropy rare-earth zirconate ceramics for thermal barrier coatings: High-temperature phase stability, thermophysical and mechanical properties,” *J. Alloys Compd.*, vol. 1010, p. 178047, Jan. 2025, doi: 10.1016/j.jallcom.2024.178047.
- [22] R. Yan *et al.*, “Mechanical, thermal and CMAS resistance properties of high-entropy (Gd_{0.2}Y_{0.2}Er_{0.2}Tm_{0.2}Yb_{0.2})₂Zr₂O₇ ceramics,” *Ceram. Int.*, vol. 49, no. 12, pp. 20729–20741, Jun. 2023, doi: 10.1016/j.ceramint.2023.03.205.
- [23] H. Chen *et al.*, “High entropy (Y_{0.2}Yb_{0.2}Lu_{0.2}Eu_{0.2}Er_{0.2})₃Al₅O₁₂: A novel high temperature stable thermal barrier material,” *J. Mater. Sci. Technol.*, vol. 48, pp. 57–62, Jul. 2020, doi: 10.1016/j.jmst.2020.01.056.